



Binary adsorption of phenol and o-Cresol from aqueous solution on date palm pits based activated carbon: a fixed-bed column study

Nuhu Dalhat Mu'azu^{a,*}, Nabeel Jarrah^{a,b}, Mohammad Hussain Essa^c

^aEnvironmental Engineering Department, University of Dammam, Dammam 31451, Saudi Arabia, Tel. +966507532689; emails: dalhat@gmail.com (N.D. Mu'azu), najarrah@ud.edu.sa (N. Jarrah)

^bChemical Engineering Department, Mutah University, Karak 61710, Jordan, Tel. +966593087655; email: najarrah@ud.edu.sa

^cDepartment of Civil and Environmental Engineering, King Fahd University of Petroleum and Minerals, Dhahran 31262, Saudi Arabia, Tel. +966507126861; email: mhessa@kfupm.edu.sa

Received 14 February 2016; Accepted 4 June 2016

ABSTRACT

In this study, binary adsorption of phenol and o-Cresol on locally produced granulated activated carbon (GAC) produced from date palm pits was investigated using continuous fixed-bed column. Experiments were conducted at $23^{\circ}\text{C} \pm 2^{\circ}\text{C}$ to evaluate the effects of the bed height (10, 15, 20, 25 and 40 cm), flow rate (5, 50 and 35 mL min⁻¹), and influent concentration of phenol and o-Cresol (10, 20 and 50 mg L⁻¹) on the breakthrough curves of phenol and o-Cresol. Thomas, Adams-Bohart, and Yoon-Nelson kinetic models were employed to understand the behavior of the fixed bed adsorption column and also to enable adequate prediction of the breakthrough curves. Fixed-column exhaustion time was found to increase when the bed height is increased, influent flow rate is decreased, and/or the influent concentration is decreased. Breakthrough experiments indicate that GAC can absorb more o-Cresol as compared with phenol, particularly at high influent concentration, flow rate, and bed height. For both phenol and o-Cresol, Thomas and Yoon-Nelson models are better in describing the experimental breakthrough data, than Adams-Bohart model. The date palm pits based GAC employed in this study has great potentials for use as an adsorbent for the binary adsorption of phenolic compounds from aqueous matrixes.

Keywords: Activated carbon; Date palm pits; Binary adsorption; Phenol and o-Cresol; Fixed bed modeling; Thomas model; Adams-Bohart model; Yoon-Nelson model

1. Introduction

Phenols are a class of aromatic compounds widely employed in many industrial processes [1,2]. However, they are listed as priority pollutants due to their varying degree of harmfulness to humans and other living organisms even at lower concentrations levels [3–5]. Environmental regulatory bodies, such as the USEPA, have set a strict limit of 0.001 ppm phenol in discharged wastewater streams [6]. Thus, the decontamination of wastewater containing phenolic compounds is crucial to lower their concentration below

the regulatory standards prior to discharge into receiving water streams. Many physicochemical technologies are available for the removal of phenolic compounds from aqueous streams and they have been comprehensively reviewed [7–10]. Adsorption using activated carbon is one of the most attractive recuperative processes for the elimination of phenolic compounds from aqueous matrixes due to its cost competitiveness [7,11,12]. Activated carbon can be produced from abundant and low cost raw materials such as agricultural solid waste. These materials contain organic compounds such as lignin, cellulose, and hemicellulose with appropriate functional groups that can be effectively bind and hold onto phenolic compounds [9,10,13]. Moreover, the

* Corresponding author.

use of solid waste to produce activated carbon has the advantage of providing a solution to the waste disposal problem as well as curtailing the exorbitant cost of adsorbents [9,10].

Ahmad et al. [14] published a comprehensive review on the potential of using granulated activated carbon (GAC) derived from raw and modified date pits, for the elimination of organic pollutants from wastewater. Several studies have demonstrated the feasibility of removing phenolic compounds using GAC from date pits, though with widely varying capacities for adsorption depending on source raw material and the activation method employed [15–19]. Merzougui and Addoun [19] investigated the single-component adsorption of phenol, p-Cresol, and o-Chlorophenol batchwise using GAC produced from date pits via KOH chemical activation. They found that the maximum adsorption capacities were 169.49, 322.58, 208.33 mg g⁻¹, respectively. Several other studies available the literature determined the single-component adsorptive capacities of phenolic compounds onto both commercial GAC and cheaper GAC produced from solid wastes with very few works carried out in continuous flow systems [9,20–22]. There are distinct advantages of higher adsorption capacity for continuous process (column studies) over batch type operations [9,23]. Additionally, practical industrial wastewater treatment processes are based on the continuous process [24,25]; hence, rendering the fixed bed study more beneficial. Eventhough, adsorption of phenolic compounds onto GAC has been studied intensively, yet, studies on the determination of adsorptive capacity of phenols in multi-component aqueous matrixes are rare [18,21,26]. To the best knowledge found in available literature, there is no study that employed date palm pits wastes based GAC for the simultaneous removal of phenol and o-Cresol in binary matrix using fixed-bed continuous system and its breakthrough modeling. Hence, the main objective of this study was to evaluate the potential of using a fixed bed of date palm pits based GAC for the simultaneous removal of phenol and o-Cresol from binary mixture in aqueous solution using Thomas, Adams–Bohart, and Yoon–Nelson kinetic models. The effect of the essential column design parameters (i.e., initial inlet concentration, flow rate bed height) on the breakthrough curves and performance were evaluated. The results of this study will be useful in designing adsorption columns for wastewater treatment using date palm pits based GAC.

2. Materials and methods

2.1. Granular activated carbon production from date palm pits

The date palm pits used for the activated carbon production were obtained from Al-Medina city, Saudi Arabia. The nominal particle size was selected as that passing 400- μ m sieve in a laboratory crusher setup and chemical activation using phosphoric acid (H₃PO₄) was employed in the activated carbon production process. Details of the production procedure of the GAC used have been reported elsewhere [27,28].

2.2. Produced activated carbon characterization

The GAC used was characterized using various analytical techniques and instruments. Total carbon content was measured using Analytik Jena Multi EX 2000 equipment

(Germany) based on procedure described elsewhere [29]. Fourier transform infrared (FTIR) spectra for were recorded by using Nicolet iS10 Spectrometer (Thermo Scientific, USA) within the region of 700–4,000 cm⁻¹. Thermo-gravimetric analyses (TGA) was performed using TGA-50 (Shimadzu, Japan) by heating 10 mg of the GAC sample at rate of 10°C min⁻¹ between 20°C and 600°C. The BET surface area and other relevant characteristics of the GAC were measured by nitrogen adsorption in a sorptometer (ASAP 2020, Micromeritics, USA), while standard scanning electron microscope (SEM, Jeol, Japan) was used for the surface morphology of the GAC was characterization.

2.3. Reagents

All the chemicals used in this study are of high purity grade (analytical) from Aldrich company. Double distilled water was used to prepare the solutions. Glassware were cleaned with chromic acid and then followed by thorough rinsing using distilled water. Phenol and o-Cresol in single stock solutions (1,000 mg L⁻¹ each) were prepared at 23°C \pm 2°C, and subsequently buffered with KH₂PO₄ to ensure neutral pH was maintained throughout the experiments.

2.4. Fixed-bed column adsorption experiments

Using 60 cm long and 2.54 cm diameter Plexiglas columns (Fig. 1) packed with the GAC sample, fixed-bed column study was performed at different bed heights of 10, 13.3, 15, 25, and 40 cm were used in this study. Solutions with a binary mixture of phenol and o-Cresol, each of same concentration (10, 20, and 50 mg L⁻¹), were fed from the top of the columns at the desired flow rate (5, 15, and 30 mL min⁻¹). In each experiment, effluent samples were taken at specified time intervals for phenol and o-Cresol residual concentration quantification. All experiments were run in duplicates and average values are reported herein.

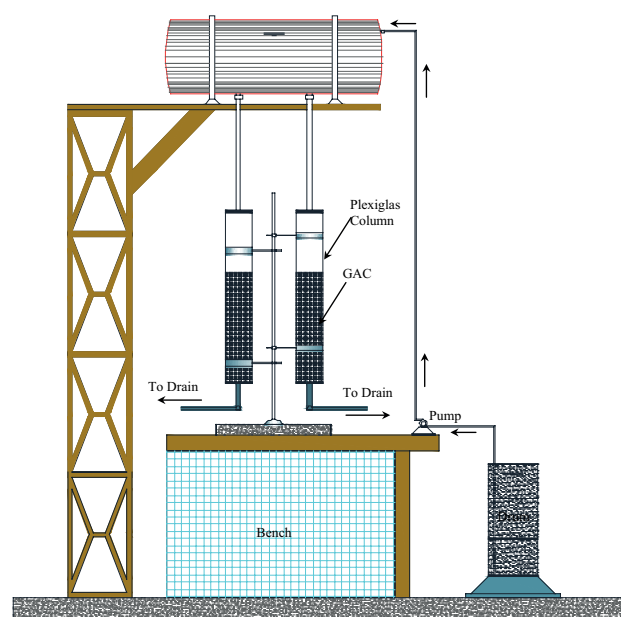


Fig. 1. Fixed-bed adsorption set-up.

2.5. Phenol and o-Cresol quantification

Concentration of phenol and o-Cresol in samples drawn from the fixed bed experiments was quantified using HPLC Ultimate 3000 (Shidmazu, Japan) equipped with photodiode array detector (Shidmazu, Japan) as per method described earlier [30].

2.6. Data analysis and breakthrough curves

Breakthrough curves were used to evaluate the performance of the fixed-bed columns towards binary adsorption of phenol and o-Cresol. Typically, a breakthrough curve is a plot of the ratio of the concentration of the adsorbate in the effluent to that of the influent (i.e., C_t/C_0) as a function of time (t) or volume of effluent (V_{eff} , mL). V_{eff} can be calculated using Eq. (1), where t_{total} (min) and Q (mL min⁻¹) represent the total flow time and the volumetric flow rate, respectively. The breakthrough point is reached when the bed becomes saturated with the adsorbate. The breakthrough point is taken as the point where C_t equals 5% of C_0 . After reaching the breakthrough point, the concentration of the adsorbate increases rapidly until it reaches the exhaustion point, where the column approaches complete saturation. The exhaustion point is the point at which C_t reaches 95% of C_0 [31–34]. The total mass adsorbed (q_{total} , mg) by the column can be obtained using Eq. (2), where $C_0 - C_t$ is represented by the concentration of the adsorbate (C_{ads}). The total mass of the adsorbate which has entered the column (m_{total} , g) is calculated using Eq. (3). The percent adsorbate removal ($Y\%$), as defined by Eq. (4), can be used to evaluate the performance of the column. The maximum column uptake capacity of the (q_{eq}) represents the capacity of the adsorbent required to remove the adsorbate, as defined by Eq. (5), where m_{GAC} (g) is the total dry weight in gram of the GAC in the column. The time taken for the solution to flow through the column or the empty bed contact time (EBCT, min) is given in Eq. (6), where V_{B} is the bed volume (mL) [34–39].

$$V_{\text{eff}} = Qt_{\text{total}} \quad (1)$$

$$q_{\text{total}} = Q / 1000 \int C_{\text{ad}} dt \quad (2)$$

$$m_{\text{total}} = C_0 Q t_{\text{total}} / 1000 \quad (3)$$

$$Y\% = q_{\text{total}} / m_{\text{total}} \times 100 \quad (4)$$

$$q_{\text{eq}} = q_{\text{total}} / m_{\text{GAC}} \quad (5)$$

$$\text{EBCT} = V_{\text{B}} / Q \quad (6)$$

2.7. Modeling of the breakthrough curve of phenol and o-Cresol adsorption

Effective design of an adsorption column essentially requires adequate kinetic modeling of the breakthrough curves of the adsorbate in the effluent. This is due to the fact that experimental evaluation of the performance of a column under different operating conditions is tedious and expensive. Consequently, there exist several mathematical models developed for determine the breakthrough curves of fixed-bed systems based on observed experimental data [37,40]. Due to their popularity and applicability without requiring

isotherm information, Thomas, Adams–Bohart, and Yoon–Nelson models were employed in this study to model the overall behavior and performance of the fixed bed columns containing date pits based GAC produced locally for the binary adsorption of phenol and o-Cresol.

2.7.1. Thomas model

Thomas model is widely used to calculate the maximum fixed bed adsorbent adsorptive capacity. The model assumes Langmuir isotherm adsorption behavior and a second-order reaction kinetics that is reversible in nature [34,41,42]. This adsorption model implies that the limiting steps in the adsorption process are not attributed to the internal and external diffusion processes [31,33,43]. Eq. (7) represents the linear form of the Thomas model (i.e., $\ln[C_0/C_t - 1]$ vs. t) from which the kinetic constants values, k_{Th} and q_0 can be estimated.

$$\ln(C_0/C_t - 1) = k_{\text{Th}} q_0 m / Q - k_{\text{Th}} C_0 t \quad (7)$$

where k_{Th} is the model's constant (mL min⁻¹ mg⁻¹), q_0 is the maximum adsorptive capacity of adsorbent (mg g⁻¹), and t is the total flow time.

2.7.2. Adams–Bohart model

The Adams–Bohart model [44] mainly describes the initial behavior of the adsorption process on the breakthrough curve and it assumes that the adsorption rate is proportional to the adsorbent adsorption capacity as well as the adsorbate concentration in solution [31,34]. This model predicts the maximum saturation concentration of the adsorbate in mg L⁻¹ (N_0). The simpler form of the Adams–Bohart model is given by Eq. (8) from which the constants, N_0 and k_{AB} can be estimated by plotting $\ln(C_0/C_t)$ versus t .

$$\ln(C_0/C_t) = k_{\text{AB}} C_0 t - k_{\text{AB}} N_0 (Z/U_0) \quad (8)$$

where k_{AB} is the Adams–Bohart kinetic constant in L mg⁻¹ min⁻¹, Z is the height of the bed in cm, and U_0 is the superficial velocity in cm min⁻¹.

2.7.3. Yoon–Nelson model

Yoon–Nelson model is the simplest of the three models as it requires no information about the adsorbate, adsorbent, or the bed. The model assumes that the rate of decrease in the adsorption of each adsorbate is proportional to the probability of its adsorption and attaining breakthrough point of the adsorbate in the matrix [34,42]. Eq. (9) describes the linearized Yoon–Nelson model, where k_{YN} is rate constant (min⁻¹) and τ is 50% adsorbate breakthrough time (min).

$$\ln(C_t / C_0 - C_t) = k_{\text{YN}} t - \tau k_{\text{YN}} \quad (9)$$

3. Results and discussion

3.1. Physical and chemical properties of the activated carbon

Table 1 summarizes some important properties of the GAC used in present study. The percent carbon content (w/w) of the GAC sample of 82% from originally 47% for the raw date

Table 1
Some characteristics of the GAC used in the study

Property of GAC	Value
^a BET surface area	1,300.27 m ² g ⁻¹
Single-point surface area	1,262.4 m ² g ⁻¹
^b BJH micropore surface area	560 m ² g ⁻¹
BJH pore volume	0.274 cm ³ g ⁻¹
Average pore width [(4 V/A) by BET]	19.54 Å
GAC carbon content (w/w)	87%
Density	0.43 g cm ⁻³

^aBrunauer–Emmett–Teller.

^bBarrett–Joyner–Halenda.

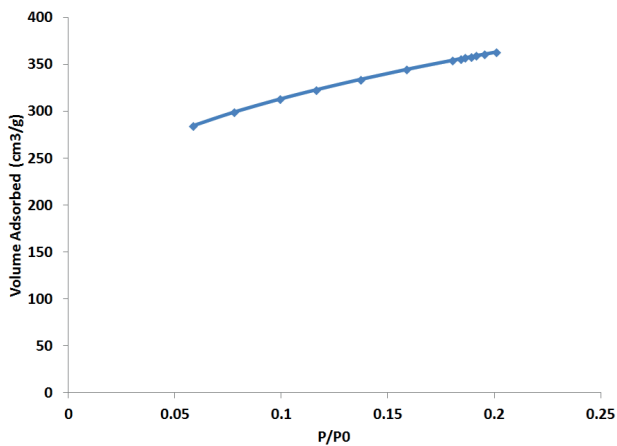


Fig. 2. Isotherm for adsorption of nitrogen onto the GAC used in the study.

palm pits, showing significant after the chemical activation [45]. The isotherm for N₂ adsorption onto the date palm pit GAC as shown in Fig. 2 shows a typical Type I adsorption trend based on Langmuir isotherms, indicating a monolayer coverage and a microporous structure. The trend in this figure hints a GAC characterized by high adsorptive capacity. Accordingly, the measured total BET surface area of the produced activated carbon was measured to be 1,300.27 m² g⁻¹, while the BJH adsorption cumulative surface area of pores between 17 and 3,000 Å was measured as 560 m² g⁻¹ at $p/p_0 = 0.2$. This high surface area corroborates the fact that H₃PO₄ is a powerful activating agent of date palm seeds. Similarly, Girgis et al. [46] and Jibril et al. [45] used date palm pit and H₃PO₄ as an activating agent to produce GAC characterized with high BET surface area of 945 and 1,100 m² g⁻¹, respectively. This implies that the optimal activation condition for the GAC used in this study yielded a higher surface area comparatively. The BJH adsorption cumulative pore volume of pores between 17 and 3,000 Å was 0.274 cm³ g⁻¹ and the BJH adsorption average pore diameter was 19.54 Å, which means that the activated carbon is microporous (i.e., pore size diameter < 20 Å or 2 nm). Fig. 3 depicts the SEM micrograph of the produced activated carbon which reveals that the surface of GAC has large pores and rough texture that are heterogeneously distributed. This indicates that there are

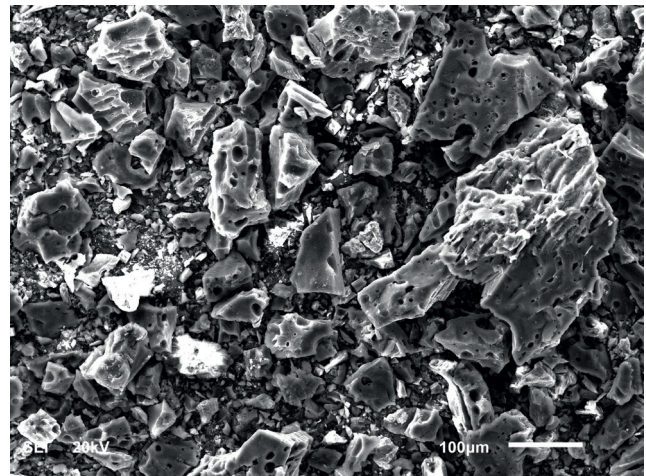


Fig. 3. SEM micrograph showing structure of the GAC used in the study.

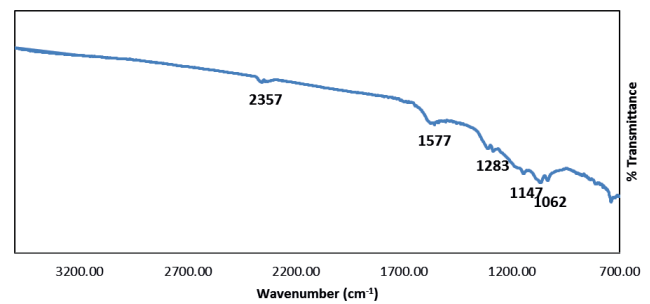


Fig. 4. FTIR spectra of the GAC used in the study.

many of micropores inside the GAC structure, hence, rendering it suitable adsorbent for removal of pollutants in water. Additionally, FTIR spectra trend (Fig. 4) revealing the surface chemistry of the GAC used evidently, shows that the GAC used possessed absorption bands and peaks of several surface functional groups. The peak at 2,357 corresponds to the presence of C-H stretching band [47] and the peak at 1,577 cm⁻¹ can be ascribed to C=O and C=C stretching vibrations [48–50]. The band at 1,283 cm⁻¹ corresponds to C-O-C stretching vibrations while peaks at 1,147 cm⁻¹ and 1,062 cm⁻¹ corresponds to the C-O stretching vibrations [51]. Bouchelta et al. [50] observed the appearance FTIR peak at 1,540 cm⁻¹ from the GAC they produced from date pits, which they ascribed it to a C=C stretch. They attributed it to high aromaticity as result of activation which renders it good for use as an adsorbent. Similarly, several other studies noted that these surface groups greatly influence GAC surface adsorption behavior [47,49,50,52].

Pyrolysis during activation of carbonaceous materials leads to residues that can be used as adsorbents with properties of the produced adsorbent depending nature of the raw materials as well as the experimental conditions. During heating, the parent material undergoes physical and chemical transformation which can be interpreted using TGA analysis. The result of the TGA test performed on the GAC sample in the range of 20°C–600°C is depicted in Fig. 5

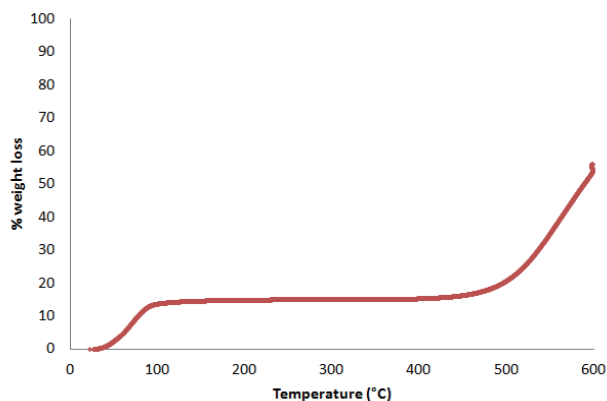


Fig. 5. TGA weight loss result Isotherm for the GAC used in the study.

to understand the weight loss during the GAC production process. Inferably, the figure indicates that no significant change in weight until beyond 500°C (the optimal temperature at which the GAC was produced). This implies that at this optimal temperature, though, most of the cellulose- and lignin-based were degraded, the active carbon component were intact, thereby, giving the observed high carbon content [29].

3.2. Effect of the influent flow rate

Figs. 6(a) and (b) display the breakthrough curves of phenol and o-Cresol, respectively. The experimental conditions are as follows: flow rates of 5, 15, and 30 mL min⁻¹; bed height of 13.3 cm; and initial concentration of each adsorbate 100 mg L⁻¹. These figures show that the breakthrough time of o-Cresol is longer than that of phenol. This indicates that more o-Cresol is adsorbed than phenol (Table 2), most likely due to the lower solubility of o-Cresol as compared with phenol at a given temperature. Fig. 6 shows that the breakthrough time for both phenol and o-Cresol decreases as the flow rate increases. Furthermore, the exhaustion time decreases when the flow rate is increased (Fig. 6(b)); however, this is not very clear cut in the case of phenol (Fig. 6(b)). The two main factors affecting the breakthrough curve are the rate of the adsorbate mass transfer to the adsorbent surface and the EBCT (i.e., the bed contact time) between the two phases. It is known that flow rate increases with Reynold number, and subsequently, the mass transfer (external) resistance decreases, accordingly. Moreover, the mass transfer coefficient increases due to the increase of the Sherwood numbers. Consequently, the adsorbate mass transfer rate from the matrix to the surface of the adsorbent increases. Therefore, both the breakthrough time and exhaustion time of the column are expected to decrease with increasing flow rate. On the other hand, increasing the flow rate led to decrease in the contact time between the adsorbate and the adsorbent, or EBCT. The results (Fig. 6 and Table 2) show that enhancing the mass transfer rate has a larger effect on the exhaustion time as well as the breakthrough time than decreasing the contact time. Similarly, Han et al. [37] suggest that the mass resistance of the external film tends to decrease

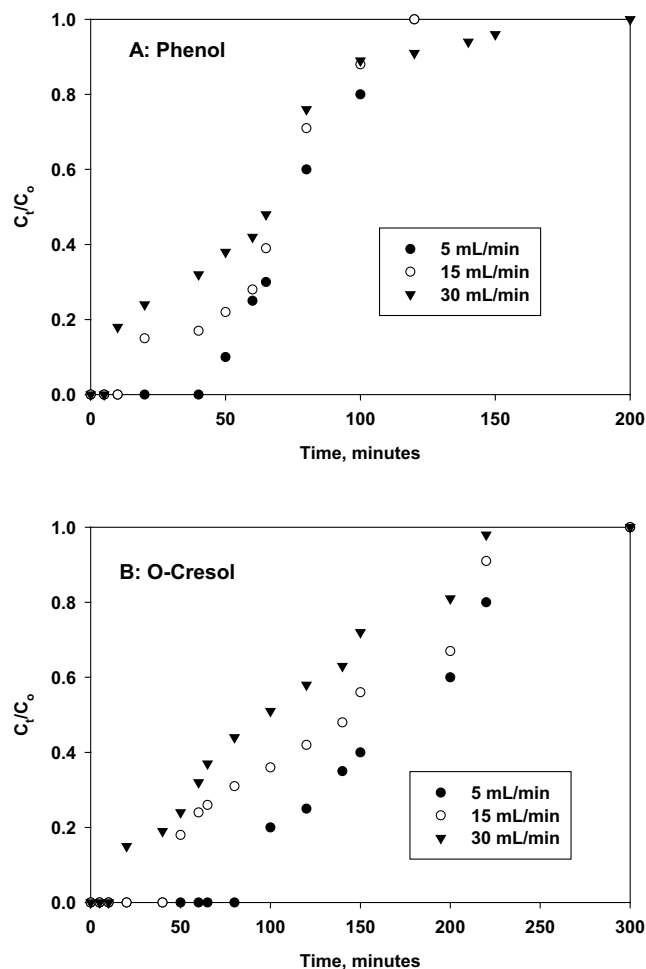


Fig. 6. Breakthrough curves for adsorption of phenol (a) and o-Cresol (b) on GAC at different flow rates (bed height, 13.3 cm; initial concentration of phenol and o-Cresol, each 100 mg L⁻¹; pH, 7; and temperature, 23°C ± 2°C).

as the flow rate becomes higher, and as a result, the saturation time decreases.

Moreover, the results in Table 2 present the dependency of adsorbent capacity on the flow rate. It can be observed that by increasing the influent flow rate from 5 to 30 mL min⁻¹, the adsorptive capacity (q_{exp}) increases from 1.21 to 5.6 mg g⁻¹ and from 2.67 to 10.27 mg g⁻¹ for phenol and o-Cresol, respectively. Obviously, the proportional increase in the adsorptive capacity (q_{eq}) with increasing flow rate was due to the availability of the adsorbate (i.e., m_{total}) (Table 2). Comparable trends have been reported elsewhere [3, 53–55]. On the other hand, the insufficient resident time of the influent decreases the bonding capacity of the pollutants onto the adsorbent [56]. The shape of the breakthrough curve steepened as the flow rate increases (Figs. 6(a) and 6(b)) which could be attributed to the adsorbate in solution having less contact time with the adsorbent as the flow rate becomes higher, which leads to a lower removal of the adsorbates. However, the shorter exhaustion time exhibited at higher flow rates increases the treatable volume (V_{eff} in Table 2). This is clearly manifested in the strong influence of the flow rate on the phenol and o-Cresol uptake capacity.

Table 2

Fixed-bed adsorption parameters for adsorption of phenol and o-Cresol on GAC from date palm pits (density = 0.43 g cm⁻³) 23°C ± 2°C and pH = 7

C_0 , mg L ⁻¹	Q , mL min ⁻¹	Z , cm	t_{total} , min	m_{total} , mg	q_{total} , mg	q_{eq} , mg g ⁻¹	V_{eff} , mL	Y , %	EBCT, min
Phenol									
100	5	13.3	120	60	35	1.21	600	58.33	13.48
100	15	13.3	120	180	89.85	3.1	1,800	49.92	4.49
100	30	13.3	200	600	162.3	5.6	6,000	27.05	2.25
10	5	10	720	36	3.65	0.17	3,600	10.13	10.14
10	5	15	720	36	3.87	0.12	3,600	10.75	15.2
10	5	25	720	36	5.96	0.11	3,600	16.54	25.33
10	5	40	720	36	7.64	0.09	3,600	21.21	40.54
10	5	13.3	640	32	13.49	0.465	3,200	42.16	13.48
20	5	13.3	480	48	19.35	0.67	2,400	40.32	13.48
50	5	13.3	360	90	30.13	1.04	1,800	33.47	13.48
o-Cresol									
100	5	13.3	300	150	77	2.67	1,500	51.33	13.48
100	15	13.3	300	450	191.03	6.61	4,500	42.45	4.49
100	30	13.3	300	900	296.85	10.27	9,000	32.98	2.25
10	5	10	600	30	3.71	0.18	3,000	12.35	10.14
10	5	15	600	30	4.44	0.14	3,000	14.78	15.2
10	5	25	600	30	6.4	0.12	3,000	21.32	25.33
10	5	40	600	30	8.23	0.09	3,000	27.42	40.54
10	5	13.3	640	32	16.66	0.57	3,200	52.06	13.48
20	5	13.3	480	48	16.66	0.57	2,400	34.71	13.48
50	5	13.3	420	105	30.37	1.05	2,100	28.92	13.48

3.3. Effect of the initial concentration

Figs. 7(a) and (b) depict the effect of the concentration of phenol and o-Cresol in the influent, respectively, on the breakthrough curves. It could be inferred from such figures that both the breakthrough and exhaustion time were attained faster when influent concentrations were high. By increasing the influent phenol concentration from 10 to 50 mg L⁻¹, the exhaustion time decreases significantly from 60 to 15 min. Meanwhile, for o-Cresol, the corresponding change is from 100 to 22 min. Hence, for both phenol and o-Cresol, the lower influent concentrations result in a longer breakthrough time as well as a larger treatable volume (Table 2). Due to the greater concentration gradient, which enhances mass transfer rate, adsorption capacity increases when influent concentration is increased [35,36]. Similarly, when the influent concentration of phenol is increased from 10 to 50 mg L⁻¹, the uptake increases from 0.465 to 1.04 mg g⁻¹, while the corresponding total mass adsorbed increases from 13.49 to 30.13 mg, respectively (Table 2). Comparable trends are also observed in the case of o-Cresol, though the uptake and corresponding total mass adsorbed are slightly higher and the breakthrough time is slightly longer than those of phenol.

3.4. Effect of the bed height

Fig. 8 shows that increasing the height of the bed produces less steep breakthrough curves and led to an increase in the exhaustion time (Table 2), while not significantly influencing the breakthrough time for both phenol and o-Cresol. The total removal of phenol and o-Cresol increased when the bed height (i.e., the mass of adsorbent) is increased. The total mass of phenol adsorbed was 3.65, 3.87, 5.96, and 7.64 mg at 10, 15, 25, and 40 cm of bed height, respectively. In the case of o-Cresol, the total mass adsorbed is slightly higher than that of phenol. The mass transfer zone which broadened due to the decrease in the slope of breakthrough curve with increasing bed height resulted in the observed improved removal of phenol and o-Cresol [57,58]. Noticeably, the increase in the bed height does not affect the treatable volume, which is mainly a function of the inflow rate and treatment time. The fixed-bed height strongly influences the uptake capacity of the adsorbent. For phenol, as shown in Table 2, the uptake capacity of 0.17, 0.12, 0.11 and 0.09 mg g⁻¹ are observed at 10, 15, 25 and 40 cm of bed height, respectively, which are quite similar to the corresponding uptake capacities for o-Cresol. The decrease in the uptake capacity with the increasing bed

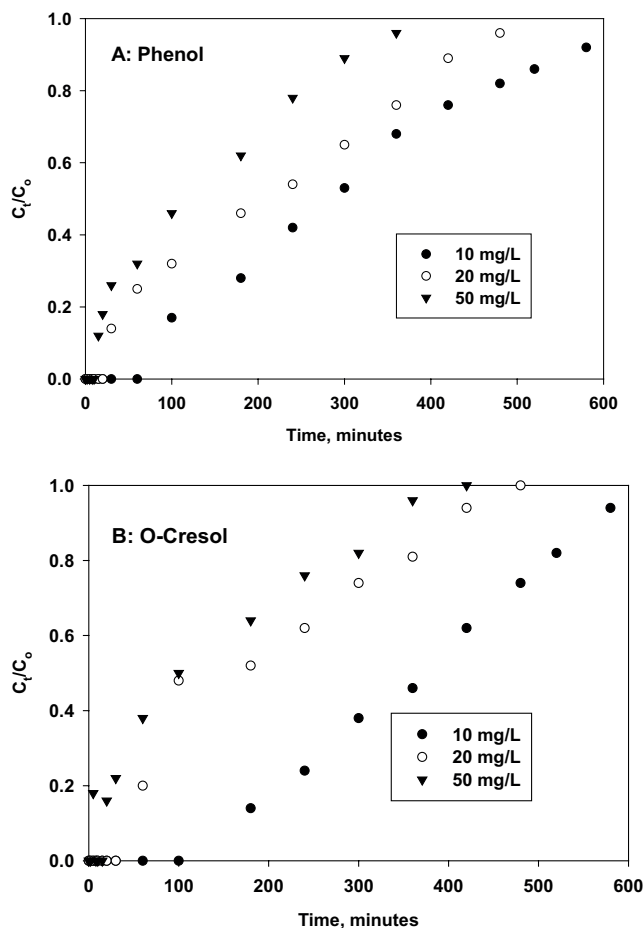


Fig. 7. Breakthrough curves for the adsorption of (a) phenol and (b) o-Cresol on GAC at different influent concentrations (bed height, 13.3 cm; flow rate, 5 mL min⁻¹; pH, 7; and temperature, 23°C ± 2°C).

height is attributed to the availability of additional mass of the adsorbent with increasing column height.

3.5. Breakthrough modeling results of phenol and o-Cresol adsorption

Analysis and prediction of breakthrough curves obtained from laboratory experiments using models is vital for the design of large-scale adsorption columns. The experimental data obtained were fitted, using regression, to three kinetic models, namely Thomas, Adams–Bohart, and Yoon–Nelson, to understand the behaviors of the adsorption process as well as determine the model that best describes the results.

3.5.1. Thomas model

Thomas model is the most popular model used to describe breakthrough curves via the estimation of the maximum adsorptive capacity of an adsorbent (mg g⁻¹). Table 3 presents the parameters of the model (i.e., k_{Th} and q_0), the correlation coefficient (R^2) and standard deviation (SD) between the Thomas model's experimental and the predicted results for both phenol and o-Cresol. The presented statistical parameters of the model's fitting, that is, R^2 as well as the SD, both indicate high quality

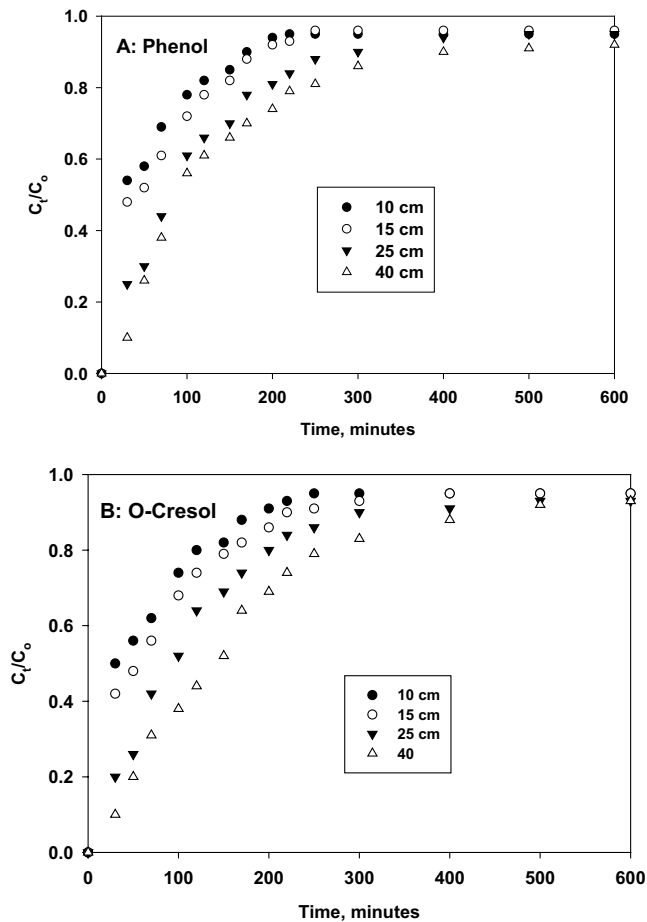


Fig. 8. Breakthrough curves for the adsorption of (a) phenol and (b) o-Cresol on GAC at different bed heights (flow rate, 5 mL min⁻¹; initial concentration of phenol and o-Cresol, 10 mg L⁻¹; initial pH, 7; and temperature, 23°C ± 2°C).

model's fitting. This is also similar to the other two employed models (i.e., Adams–Bohart and Yoon–Nelson) as presented under respective headings in subsections below. Table 3 shows that when influent concentration is increased, the value of q_0 increases and the value of k_{Th} decreases. As discussed above, the value of q_0 increases due to the rise in the driving force (i.e., difference adsorbate concentration in solution and on the surface of the adsorbent) of mass transfer [34]. The model also predicts that when the bed height and/or flow rate is increased, the value of q_0 increases and the value of k_{Th} decreases. This model predictions agree well with the experimental results discussed earlier, showing that lower flow rates, higher influent concentrations, and higher bed heights enhance the adsorption ability of a fixed-bed column. Most values of R^2 are higher than 0.9, indicating good description of the column data by the Thomas model for both phenol and o-Cresol. Thomas model has been shown to be more suitable for cases where the adsorption process is not controlled by mass transfer [34,37].

3.5.2. Adams–Bohart model

The breakthrough data for phenol and o-Cresol were used to perform linear regression in the form of $\ln C_t/C_0$ vs. t to

Table 3
Model parameters obtained by fitting breakthrough data to the Thomas model using linear regression

C_0 mg L ⁻¹	Q mL min ⁻¹	Z , cm	Phenol				o-Cresol			
			$k_{Th} \times 10^4$ mL min ⁻¹ mg ⁻¹	q_0 mg g ⁻¹	R^2	SD ^a	$k_{Th} \times 10^4$ mL min ⁻¹ mg ⁻¹	q_0 mg g ⁻¹	R^2	SD ^a
100	5	13.3	7.05	11,820.33	0.977	0.2110	2.18	15,290.52	0.969	0.1796
100	15	13.3	5.02	16,600.27	0.893	0.4540	1.82	18,315.02	0.917	1.9897
100	30	13.3	3.55	14,084.51	0.967	0.3054	2.29	14,556.04	0.907	0.4647
10	5	10	14.8	938.43	0.991	0.0937	13.50	1,234.568	0.991	0.0872
10	5	15	14.8	938.45	0.995	0.0745	9.40	1,773.05	0.929	0.2821
10	5	25	11.7	1,187.09	0.937	0.6414	9.50	1,754.386	0.872	0.3831
10	5	40	7.00	1,984.13	0.852	0.3916	9.00	1,851.852	0.923	0.2423
10	5	13.3	9.10	1,717.03	0.971	0.2780	10.5	1,488.095	0.977	0.2233
20	5	13.3	4.85	4,295.53	0.965	0.2931	4.70	4,432.624	0.922	0.3631
50	5	13.3	2.64	10,521.89	0.979	0.2476	2.40	9,920.635	0.952	0.3482

^aStandard deviation.

Table 4
Model parameters obtained by fitting breakthrough data to the Adams–Bohart model using linear regression

C_0 mg L ⁻¹	Q mL min ⁻¹	Z cm	Phenol					o-Cresol				
			$k_{ab} \times 10^4$ L mg ⁻¹ min ⁻¹	U_0 cm min ⁻¹	N_0 mg L ⁻¹	R^2	SD	$k_{ab} \times 10^4$ L mg ⁻¹ min ⁻¹	U_0 cm min ⁻¹	N_0 mg L ⁻¹	R^2	SD ^a
100	5	13.3	3.93	0.987	739.28	0.886	0.2749	1.12	0.987	1,773.54	0.985	0.0644
100	15	13.3	2.53	2.960	2,306.73	0.931	0.1804	8.30	2.960	5,150.80	0.960	0.0998
100	30	13.3	1.21	5.919	5,866.52	0.899	0.1905	0.870	5.919	8,977.21	0.885	0.2005
10	5	10	2.90	0.987	212.66	0.906	0.0634	2.90	0.987	229.26	0.897	0.0727
10	5	15	3.20	0.987	150.25	0.904	0.0773	3.40	0.987	139.26	0.882	0.0859
10	5	25	2.80	0.987	114.56	0.817	0.2546	3.20	0.987	113.37	0.851	0.2916
10	5	40	2.20	0.987	91.31	0.733	0.4835	3.20	0.987	89.83	0.804	0.4092
10	5	13.3	3.10	0.987	415.31	0.884	0.1967	4.10	0.987	431.60	0.926	0.1688
20	5	13.3	1.65	0.987	577.56	0.936	0.2113	1.10	0.987	669.91	0.982	0.2849
50	5	13.3	9.00	0.987	1,207.64	0.901	0.3034	7.60	0.987	1,251.29	0.859	0.2848

^aStandard deviation.

determine the respective values for the Adams–Bohart models constants. The values of k_{AB} and N_0 along with the values of R^2 are presented in Table 4. When the flow rate is increased, the value of k_{AB} decreases; when bed height is increased, the value of N_0 increases (Table 4). This suggests that mass transfer is dominating the adsorption kinetics at the initial part of the column [34,57]. However, a clear trend cannot be identified in the other values. The regression coefficients for all the fitted breakthrough data indicate good correlation ($R^2 = 0.8039–0.9847$), suggesting that the model predicts the experimental results well. However, Thomas model predicts the experimental data better than the Adams–Bohart model. This can be attributed to the fact that Adams–Bohart model is applicable to the initial part of the breakthrough curve. Moreover, the model is more suitable for the prediction of

adsorption with a surface reaction, which does not seem to be the case in this study.

3.5.3. Yoon–Nelson model

Table 5 presents the values of the parameters of the Yoon–Nelson Model (i.e., k_{YN} and the τ) along with the correlation coefficient R^2 obtained by fitting the breakthrough data to the model using linear regression. Evidently, the value of τ decreases when the height of the bed is decreased, the flow rate is increased, or the influent concentration is increased. This corroborates the fact that fixed column saturation occurs more rapidly at higher concentration, higher flow rate, and/or with a short bed [24]. Similar to the Thomas model, most values of R^2 are higher than 0.9, which indicates that the

Table 5
Model parameters obtained by fitting breakthrough data to the Yoon–Nelson model using linear regression

C_0 mg L ⁻¹	Q mL min ⁻¹	Z cm	Phenol				o-Cresol			
			$k_{yn} \times 10^4$ min ⁻¹	τ min	R^2	SD	$k_{yn} \times 10^4$ min ⁻¹	τ min	R^2	SD ^a
100	5	13.3	705	77.67	0.977	0.2110	183	175.87	0.993	0.2421
100	15	13.3	502	68.08	0.894	0.4540	182	130.49	0.917	0.3212
100	30	13.3	355	57.56	0.967	0.3054	229	99.06	0.908	0.4647
10	5	10	148	20.91	0.991	0.0937	138	6.75	0.990	0.0900
10	5	15	148	39.27	0.996	0.6541	94	26.8	0.930	0.4596
10	5	25	86	72.50	0.877	0.4499	83	89.60	0.826	0.5324
10	5	40	57	63.40	0.822	0.4503	83	140.63	0.908	0.4798
10	5	13.3	91	285.98	0.971	0.2780	105	358.97	0.978	0.2233
20	5	13.3	0.97	201.32	0.966	0.2931	0.94	172.11	0.923	0.3631
50	5	13.3	1.32	131.61	0.980	0.2476	1.2	129.41	0.952	0.3482

^aStandard deviation.

Yoon–Nelson model also adequately describes the column data for both phenol and o-Cresol.

Interestingly, all three models used in this study describe the results well for binary adsorption of phenol and o-Cresol on GAC, even though these models were derived based on single component adsorption. However, Adams–Bohart model requires more parameters and is not as good as the other two models. On the other hand, Yoon–Nelson model requires the least number of parameters and provides information about the time required to reach 50% saturation, which can shorten the duration of an experiment.

4. Conclusion

The binary adsorption of phenol and o-Cresol from aqueous solution was studied in a continuous fixed-bed column of granular activated carbon produced from date palm pits. Adams–Bohart, Thomas, and Yoon–Nelson kinetic models were employed to understand the performance of the adsorption column and also to predict the breakthrough curves. The effect of the flow rate, initial concentration, and bed height on the breakthrough curves was evaluated. The adsorption capacity of GAC towards o-Cresol is higher than that of phenol. The increase in the flow rate and initial concentration speeded up the exhaustion of the column. On the other hand, the increase in the bed height slowed down the exhaustion of the column. Both Thomas and Yoon–Nelson models describe the breakthrough curves of both phenol and o-Cresol very well, suggesting that these models can be used for column design purposes during binary adsorption of the two compounds. This study demonstrates that GAC obtained from date palm pits is suitable for binary removal of phenol and o-Cresol from wastewater streams.

Acknowledgments

The authors would like to acknowledge the support provided by King Abdul-Aziz City for Science and Technology (KACST) through the Deanship of Scientific Research (DSR)

of University of Dammam (UoD) for funding this work through Project No. 12-Env2229-46 as part of the National Science, Technology and Innovation Plan (NSTIP).

References

- [1] H.H.P. Fang, O.-C. Chan, Toxicity of phenol towards anaerobic biogranules, *Water. Res.*, 31 (1997) 2229–2242.
- [2] F.A. Banat, B. Al-Bashir, S. Al-Asheh, O. Hayajneh, Adsorption of phenol by bentonite, *Environ. Pollut.*, 107 (2000) 391–398.
- [3] S.K. Maji, A. Pal, T. Pal, A. Adak, Modeling and fixed bed column adsorption of As (III) on laterite soil, *Sep. Sci. Technol.*, 56 (2007) 284–290.
- [4] ATSDR, Agency for Toxic Substances and Disease Registry: Priority List of Hazardous Substances, in, Atlanta, USA, <http://www.atsdr.cdc.gov/2011>.
- [5] H.S. Ibrahim, T.S. Jamil, E.Z. Hegazy, Application of zeolite prepared from Egyptian kaolin for the removal of heavy metals: II. Isotherm models, *J. Hazard. Mater.*, 182 (2010) 842–847.
- [6] USEPA, Edition of the Drinking Water Standards and Health Advisories, Washington, DC, 2006, p. 6.
- [7] G. Busca, S. Berardinelli, C. Resini, L. Arrighi, Technologies for the removal of phenol from fluid streams: a short review of recent developments, *J. Hazard. Mater.*, 160 (2008) 265–288.
- [8] C. Guohua, Electrochemical technologies in wastewater treatment, *Sep. Sci. Technol.*, 38 (2004) 11–41.
- [9] M. Ahmaruzzaman, Adsorption of phenolic compounds on low-cost adsorbents: a review, *Adv. Colloid Interface Sci.*, 143 (2008) 48–67.
- [10] S.-H. Lin, R.-S. Juang, Adsorption of phenol and its derivatives from water using synthetic resins and low-cost natural adsorbents: a review, *J. Environ. Manage.*, 90 (2009) 1336–1349.
- [11] N.N. Dutta, S. Borthakur, R. Baruah, A novel process for recovery of phenol from alkaline wastewater: laboratory study and predesign cost estimate, *Water Environ. Res.*, 70 (1998) 4–9.
- [12] M.L. Soto, A. Moure, H. Domínguez, J.C. Parajó, Recovery, concentration and purification of phenolic compounds by adsorption: a review, *J. Food Eng.*, 105 (2011) 1–27.
- [13] A. Dąbrowski, P. Podkościelny, Z. Hubicki, M. Barczak, Adsorption of phenolic compounds by activated carbon—a critical review, *Chemosphere*, 58 (2005) 1049–1070.
- [14] T. Ahmad, M. Danish, M. Rafatullah, A. Ghazali, O. Sulaiman, R. Hashim, M. Ibrahim, The use of date palm as a potential adsorbent for wastewater treatment: a review, *Environ. Sci. Pollut. Res.*, 19 (2012) 1464–1484.

- [15] F. Banat, S. Al-Asheh, L. Al-Makhadmeh, Utilization of raw and activated date pits for the removal of phenol from aqueous solutions, *Chem. Eng. Technol.*, 27 (2004) 80–86.
- [16] Y.A. Alhamed, Activated Carbon from Dates' Stone by ZnCl₂ Activation, *JKAU: Eng. Sci.*, 17 (2006) 75–98.
- [17] Y.A. Alhamed, Adsorption kinetics and performance of packed bed adsorber for phenol removal using activated carbon from dates' stones, *J. Hazard. Mater.*, 170 (2009) 763–770.
- [18] A.Y. Okasha, H.G. Ibrahim, Phenol removal from aqueous systems by sorption of using some local waste materials, *EJEAFChE*, 9 (2010) 796–807.
- [19] Z. Merzougui, F. Addoun, Effect of oxidant treatment of date pit activated carbons application to the treatment of waters, *Desalination*, 222 (2008) 394–403.
- [20] A.E. Vasu, Removal of phenol and o-Cresol by adsorption onto activated carbon, *J. Chem.*, 5 (2008) 224–232.
- [21] M.A. Hassan, H.M. Eissa, A.M. Mohammed, Adsorption of phenol and o-Cresol from dilute aqueous solution on bentonite clay, *J. Int. Environ. Appl. Sci.*, 6 (2011) 547–552.
- [22] V.V. Daniel, B.B. Gulyani, B.G. Prakash Kumar, Usage of date stones as adsorbents: a review, *J. Disper. Sci. Technol.*, 33 (2012) 1321–1331.
- [23] M. Ahmaruzzaman, D.K. Sharma, Adsorption of phenols from wastewater, *J. Colloid. Interface. Sci.*, 287 (2005) 14–24.
- [24] M. Calero, F. Hernáinz, G. Blázquez, G. Tenorio, M. Martín-Lara, Study of Cr (III) biosorption in a fixed-bed column, *J. Hazard. Mater.*, 171 (2009) 886–893.
- [25] S. Baral, N. Das, T. Ramulu, S. Sahoo, S. Das, G.R. Chaudhury, Removal of Cr (VI) by thermally activated weed *Salvinia cucullata* in a fixed-bed column, *J. Hazard. Mater.*, 161 (2009) 1427–1435.
- [26] C. Quintelas, E. Sousa, F. Silva, S. Neto, T. Tavares, Competitive biosorption of ortho-Cresol, phenol, chlorophenol and chromium (VI) from aqueous solution by a bacterial biofilm supported on granular activated carbon, *Process Biochem.*, 41 (2006) 2087–2091.
- [27] S. Lukman, M.H. Essa, N.D. Mu'azu, A. Bukhari, C. Basheer, Adsorption and desorption of heavy metals onto natural clay material: influence of initial pH, *J. Environ. Sci. Technol.*, 6 (2013) 1–15.
- [28] M.H. Essa, M.A. Al-Zahrani, T.N. Suresh, Optimization of activated carbon production from date pits, *Int. J. Environ. Eng.*, 5 (2013) 325–338.
- [29] M.S. Vohra, Adsorption-based removal of gas-phase benzene using granular activated carbon (GAC) produced from date palm pits, *Arab. J. Sci. Eng.*, 40 (2015) 3007–3017.
- [30] N.D. Mu'azu, M.H. Al-Malack, N. Jarrah, Electrochemical oxidation of low phenol concentration on boron doped diamond anodes: optimization via response surface methodology, *Desal. Wat. Treat.*, 52 (2014) 7293–7305.
- [31] R. Han, Y. Wang, X. Zhao, Y. Wang, F. Xie, J. Cheng, M. Tang, Adsorption of methylene blue by phoenix tree leaf powder in a fixed-bed column: experiments and prediction of breakthrough curves, *Desalination*, 245 (2009) 284–297.
- [32] S. Kundu, S.S. Kavalakatt, A. Pal, S.K. Ghosh, M. Mandal, T. Pal, Removal of arsenic using hardened paste of Portland cement: batch adsorption and column study, *Water. Res.*, 38 (2004) 3780–3790.
- [33] S.S. Baral, N. Das, T.S. Ramulu, S.K. Sahoo, S.N. Das, G.R. Chaudhury, Removal of Cr(VI) by thermally activated weed *Salvinia cucullata* in a fixed-bed column, *J. Hazard. Mater.*, 161 (2009) 1427–1435.
- [34] S. Chen, Q. Yue, B. Gao, Q. Li, X. Xu, K. Fu, Adsorption of hexavalent chromium from aqueous solution by modified corn stalk: a fixed-bed column study, *Bioresour. Technol.*, 113 (2012) 114–120.
- [35] M. Tamez Uddin, M. Rukanuzzaman, M. Maksudur Rahman Khan, M. Akhtarul Islam, Adsorption of methylene blue from aqueous solution by jackfruit (*Artocarpus heterophyllus*) leaf powder: a fixed-bed column study, *J. Environ. Manage.*, 90 (2009) 3443–3450.
- [36] N. Chen, Z. Zhang, C. Feng, M. Li, R. Chen, N. Sugiura, Investigations on the batch and fixed-bed column performance of fluoride adsorption by Kanuma mud, *Desalination*, 268 (2011) 76–82.
- [37] R. Han, L. Zou, X. Zhao, Y. Xu, F. Xu, Y. Li, Y. Wang, Characterization and properties of iron oxide-coated zeolite as adsorbent for removal of copper(II) from solution in fixed bed column, *Chem. Eng. J.*, 149 (2009) 123–131.
- [38] E. Oguz, M. Ersoy, Biosorption of cobalt(II) with sunflower biomass from aqueous solutions in a fixed bed column and neural networks modelling, *Ecotoxicol. Environ. Saf.*, 99 (2014) 54–60.
- [39] S. Netpradit, P. Thiravetyan, S. Towprayoon, Evaluation of metal hydroxide sludge for reactive dye adsorption in a fixed-bed column system, *Water. Res.*, 38 (2004) 71–78.
- [40] P.A. Kumar, S. Chakraborty, Fixed-bed column study for hexavalent chromium removal and recovery by short-chain polyaniline synthesized on jute fiber, *J. Hazard. Mater.*, 162 (2009) 1086–1098.
- [41] D. Liu, D. Sun, Simulation of indigo carmine dye adsorption on polymer doped sawdust in fixed-bed systems, *Desal. Wat. Treat.*, 27 (2011) 285–293.
- [42] K.Z. Setshedi, M. Bhaumik, M.S. Onyango, A. Maity, Break-through studies for Cr(VI) sorption from aqueous solution using exfoliated polypyrrole-organically modified montmorillonite clay nanocomposite, *J. Ind. Eng. Chem.*, 20 (2014) 2208–2216.
- [43] Z. Aksu, F. Gönen, Biosorption of phenol by immobilized activated sludge in a continuous packed bed: prediction of breakthrough curves, *Process Biochem.*, 39 (2004) 599–613.
- [44] G. Bohart, E. Adams, Some aspects of the behavior of charcoal with respect to chlorine, *J. Am. Chem. Soc.*, 42 (1920) 523–544.
- [45] B. Jibril, O. Houache, R. Al-Maamari, B. Al-Rashidi, Effects of H₃PO₄ and KOH in carbonization of lignocellulosic material, *J. Anal. Appl. Pyrol.*, 83 (2008) 151–156.
- [46] B.S. Girgis, A.-N.A. El-Hendawy, Porosity development in activated carbons obtained from date pits under chemical activation with phosphoric acid, *Micropor. Mesopor. Mater.*, 52 (2002) 105–117.
- [47] K. Riahi, B.B. Thayer, A.B. Mammou, A.B. Ammar, M.H. Jaafoura, Biosorption characteristics of phosphates from aqueous solution onto Phoenix *dactylifera* L. date palm fibers, *J. Hazard. Mater.*, 170 (2009) 511–519.
- [48] A.P. Craig, A.S. Franca, L.S. Oliveira, Evaluation of the potential of FTIR and chemometrics for separation between defective and non-defective coffees, *Food Chem.*, 132 (2012) 1368–1374.
- [49] A. Daifullah, B. Girgis, Impact of surface characteristics of activated carbon on adsorption of BTEX, *Colloids Surf., A*, 214 (2003) 181–193.
- [50] C. Bouchelta, M.S. Medjram, O. Bertrand, J.-P. Bellat, Preparation and characterization of activated carbon from date stones by physical activation with steam, *J. Anal. Appl. Pyrol.*, 82 (2008) 70–77.
- [51] M.-W. Jung, K.-H. Ahn, Y. Lee, K.-P. Kim, J.-S. Rhee, J.T. Park, K.-J. Paeng, Adsorption characteristics of phenol and chlorophenols on granular activated carbons (GAC), *Microchem. J.*, 70 (2001) 123–131.
- [52] A. Veksha, E. Sasaoka, M.A. Uddin, The influence of porosity and surface oxygen groups of peat-based activated carbons on benzene adsorption from dry and humid air, *Carbon*, 47 (2009) 2371–2378.
- [53] V. Vinodhini, N. Das, Packed bed column studies on Cr (VI) removal from tannery wastewater by neem sawdust, *Desalination*, 264 (2010) 9–14.
- [54] I.A. Aguayo-Villarreal, A. Bonilla-Petriciolet, V. Hernández-Montoya, M.A. Montes-Morán, H.E. Reynel-Avila, Batch and column studies of Zn²⁺ removal from aqueous solution using chicken feathers as sorbents, *Chem. Eng. J.*, 167 (2011) 67–76.
- [55] S. Kundu, A. Gupta, Analysis and modeling of fixed bed column operations on As (V) removal by adsorption onto iron oxide-coated cement (IOCC), *J. Colloid. Interface. Sci.*, 290 (2005) 52–60.
- [56] G. Yan, T. Viraraghavan, Heavy metal removal in a biosorption column by immobilized *M. rouxii* biomass, *Bioresour. Technol.*, 78 (2001) 243–249.
- [57] A.A. Ahmad, B.H. Hameed, Fixed-bed adsorption of reactive azo dye onto granular activated carbon prepared from waste, *J. Hazard. Mater.*, 175 (2010) 298–303.
- [58] J. Song, W. Zou, Y. Bian, F. Su, R. Han, Adsorption characteristics of methylene blue by peanut husk in batch and column modes, *Desalination*, 265 (2011) 119–125.